ELSEVIER

Palaeogeography, Palaeoclimatology, Palaeoecology 193 (2003) 249–260

PALAEO

www.elsevier.com/locate/palaeo

Hydrologic and geologic factors that influenced spatial variations in loess deposition in China during the last interglacial–glacial cycle: results from proxy climate and GCM analyses

Dean Rokosh [a,*], Andrew B.G. Bush [a], Nathaniel W. Rutter [a], Zhongli Ding [b,c], Jimin Sun [b,c]

[a] *Institute of Geophysics, Department of Physics, P412 Avadh Batia Physics Laboratory, Edmonton, AB, Canada T6G 2J1*
[b] *Department of Earth and Atmospheric Sciences, University of Alberta, Edmonton, AB, Canada*
[c] *Academy of Sciences, Beijing, PR China*

Received 2 October 2000; accepted 6 January 2003

Abstract

Results from climate proxy and General Circulation Model (GCM) analyses suggest that variations in soil moisture and desert expansion are key hydrologic and geologic factors, respectively, influencing temporal and spatial variations in loess texture and distribution in the Loess Plateau of China. During the last glacial period a reduction in soil moisture led to dune destabilization and a southward expansion of the desert (the source of loess) toward the Loess Plateau. Changes in soil moisture in East Asia may have been influenced by the size and extent of the Fennoscandian ice sheet, and the atmospheric circulation pattern that it induced downstream. These results suggest that both regional factors (i.e. changes in soil moisture and the position of the desert margin) and hemispherical factors (i.e. changes in the size and extent of the Eurasian ice sheets) have influenced loess deposition on the Loess Plateau of China.

Keywords: loess; desert; China; Last Glacial Maximum; General Circulation Model; soil moisture; Eurasian ice sheet

1. Introduction

On the Loess Plateau of China, the basic geologic and climatic model explaining loess deposition during former cold and warm periods is that loess grains are coarser and beds thicker during glacial periods compared to interglacial periods (Liu, 1985; An et al., 1991a,b; Ding et al., 1995; Shackleton et al., 1995; Vandenberghe et al., 1997). According to this model, loess deposition continues during interglacial periods but at reduced rates. Using these observations as a guide, the two main paleoclimatic mechanisms that have affected glacial and interglacial variations in loess deposition are: (1) variations in

* Corresponding author. Tel.: +1-780-492-4126; Fax: +1-780-492-0714.
E-mail addresses: drokosh@phys.ualberta.ca (D. Rokosh), nat.rutter@ualberta.ca (N.W. Rutter).

0031-0182/03/$ – see front matter
doi:10.1016/S0031-0182(03)00228-1

insolation received (e.g. An et al., 1991a), and (2) global ice volume variations (e.g. Liu and Ding, 1993; Ding et al., 1995; Shackleton et al., 1995). However, these paleoclimatic forcing mechanisms were interpreted using a simple, geologic model based solely on temporal variations in loess grain size and accumulation rates that assumes that the temporal variations are equally valid spatially. More recently, Rokosh (2001) suggested that temporal variations in loess grain size and accumulation rates are not representative of spatial variations in these properties. Loess grain size, thickness and accumulation rates in the Loess Plateau were compared for the last interglacial and glacial periods, resulting in a new model of loess deposition that contains both spatial and temporal components. According to this model, loess deposition is best interpreted as part of a desert–loess depositional system where sediment texture (Ding et al., 1999) and loess distribution are largely controlled by desert expansion and contraction, during cold and warm periods, respectively. In this two-compartment model, a comparison of the last interglacial and glacial depositional systems shows that there is very little difference between these systems in terms of the size of loess grains, the thickness and geometry of the beds, and loess accumulation rates. However, the principal distinction between the last glacial and interglacial depositional systems is that the distribution of loess is different, owing to desert expansion and contraction during glacial and interglacial periods, respectively. Glacial to interglacial variations in ice volume, therefore, result in a change in the distribution of loess through desert expansion and contraction, rather than having a direct influence on variations in grain size or accumulation rates. Thus, variations in global ice volume have exerted a less direct influence on variations in Chinese loess grain size, thickness and accumulation rates than has previously been assumed.

In this paper we use a new model of loess deposition and results from a coupled ocean–atmosphere General Circulation Model (GCM) analysis to determine the influence of hydrologic and geologic factors on glacial to interglacial variations in loess deposition. We take a four-fold approach to our analyses, as follows. (1) We review the links between variations in insolation, ice volume and loess deposition during the last interglacial–glacial cycle. (2) We review a new model of loess deposition during the last interglacial–glacial cycle, using results from a north to south transect of the Loess Plateau (Fig. 1). The geologic and climatic controls on spatial and temporal variations in loess deposition are outlined. (3) We examine climatic and hydrologic factors that influence modern loess deposition in North China in order to gain insight into the controls on dust deposition during the last interglacial period and, possibly, the last glacial period. (4) We generate a numerical simulation of soil moisture during the Last Glacial Maximum (LGM) in East Asia using the coupled GCM (Bush and Philander, 1999), and determine the factors that influence interglacial to glacial variations in soil moisture.

2. Methods

The grain size and magnetic susceptibility of loess and paleosol samples from seven sites were determined from the central Loess Plateau (Fig. 1). Samples were taken every 5–10 cm in the L1 loess bed and every 2–5 cm in the S1 paleosol. A smaller sample interval was used in thinner loess beds at the southern end of the transect. Grain size analysis was performed using a PRO-700 SK Laser Micron Sizer. An analysis of 20 replicate samples indicated a precision of 3.5%. Organic material, pedogenic iron and carbonates were removed prior to analysis. Bulk magnetic susceptibility was determined using a Bartington MS II susceptibility meter at the Academy of Sciences in Beijing. Susceptibility values represent one reading on an approximately 50 g bagged sample. The values are volume-specific and are presented as carbonate-free by calibrating each sample to the amount of carbonate present using the formula:

$$A2 = A1(100/(100-C))$$

where $A1$ and $A2$ are the measured and resultant magnetic susceptibility, respectively, and C is the wt% carbonate.

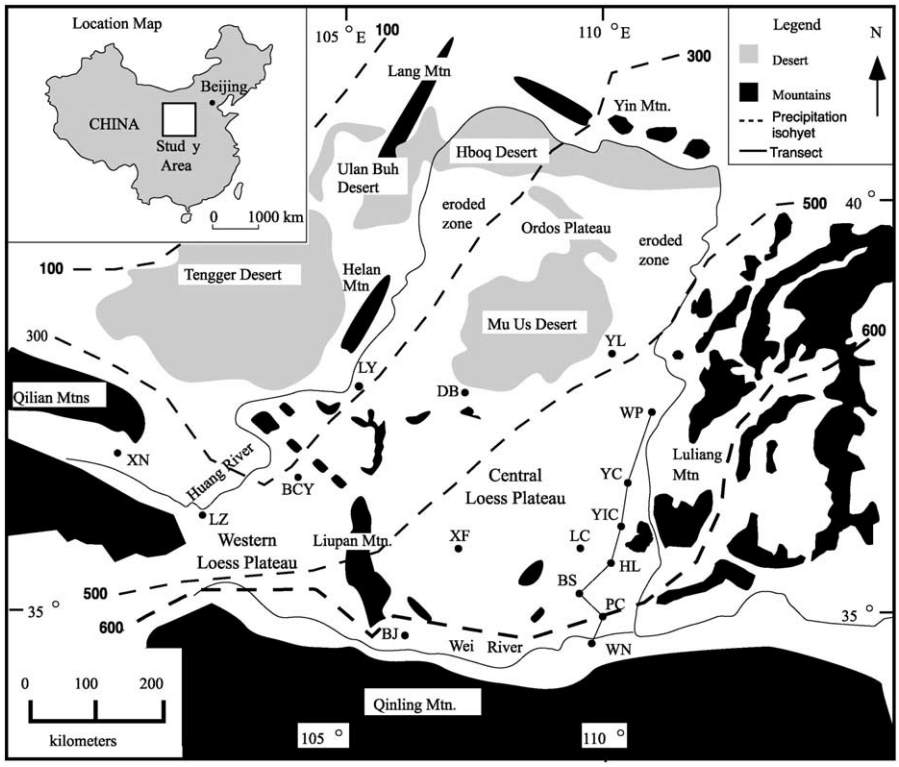

Central Loess Plateau				Western Loess Plateau	
BJ	Baoji	BS	Baishui	BCY	Baicouyuan
DB	Ding Bien	HL	Huanglong	LZJ	Lanzhou (JZT)
LC	Luochuan	LJY	Lija Yuan	LZG	Lanzhuo (GLS)
PC	Pucheng	WN	Weinan	XN	Xining
WP	Wupu	XF	Xifeng		
YC	Yanchang	YIC	Yichuan		
YL	Yulin				

Fig. 1. Map of the Loess Plateau showing the sites mentioned in the text. The base map was modified from U.S. Defense Mapping Agency Aerospace Center (1987).

Age control is determined by correlation with the age model of Liu et al. (1995), developed at Weinan at the south end of the transect (Fig. 1). The chronology of this model spans the last ca. 130 kyr and is based on accelerator mass spectrometry (AMS) measurements on radiocarbon and on thermoluminescence (TL) measurements of loess and paleosols. Loess–paleosol alternations were correlated with Marine Oxygen Isotope Stages (MIS) (Liu, 1985; Kukla, 1987a,b; Liu et al., 1995), where MIS 2, 3 and 4 (last glacial period) correspond with the Malan loess (L1), and MIS 5 (last interglacial period) corresponds with paleosol S1 (Fig. 2). The Malan loess is further subdivided in this paper into members L1-1 to L1-5, where L1-1 corresponds to MIS 2, while L1-2, 3 and 4 corrrespond with MIS 3, and L1-5 with MIS 4.

3. Comparison of loess and susceptibility records with global ice volume and insolation variations during the last interglacial–glacial cycle

Grain size and susceptibility records from Wupu and Yanchang in the Loess Plateau (Figs.

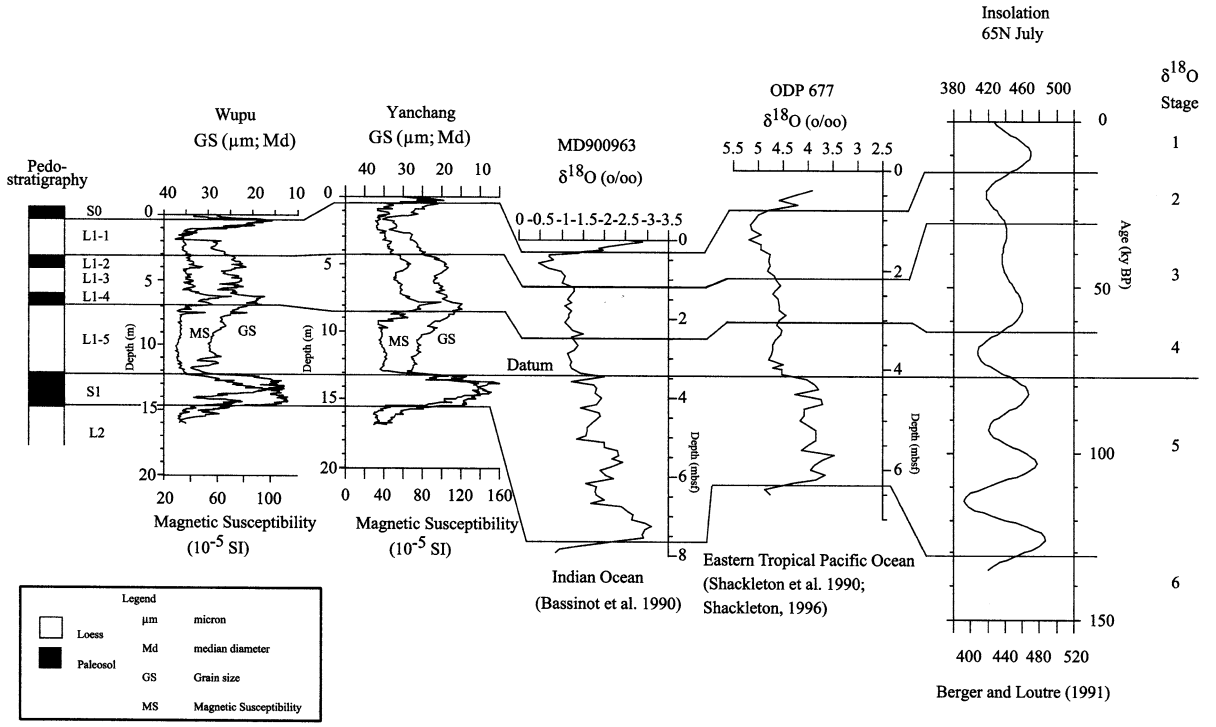

Fig. 2. Comparison of loess–paleosol stratigraphy with $\delta^{18}O$ records from the Indian and Pacific oceans. The Berger and Loutre (1991) insolation values are calculated relative to the 1950 AD value of 427 W/m^2.

1 and 2) are compared with oceanic $\delta^{18}O$ curves and a top-of-the-atmosphere insolation record from Berger and Loutre (1991). The $\delta^{18}O$ records are from the Maldives Ridge (core MD900963; latitude 05°03.30′N, longitude 73°52.60′E) of the tropical Indian Ocean (Bassinot et al., 1994), and ODP 677 in the eastern equatorial Pacific Ocean (Shackleton et al., 1990; Shackleton, 1996; latitude 1°12′N, longitude 83°44′W). The glacial to interglacial variation in $\delta^{18}O$ from core MD900963 may have been influenced by a local salinity change, which Bassinot et al. (1994) suggest was most likely controlled by changes in monsoon intensity.

In Fig. 2, the stratigraphy of the last glaciation is interpreted as alternating loess beds (L1-1, L1-3, and L1-5) and paleosols (L1-2 and L1-4). The insolation curve exhibits three periods of relatively reduced insolation intensity and two periods of increased intensity during the last glaciation (e.g. Berger and Loutre, 1991). Insolation and grain size variations are inversely correlated, while the susceptibility profile is linearly correlated with insolation during this period. The loess–paleosol variations correspond very well with the curve of Berger and Loutre (1991), showing periods of relatively reduced insolation intensity corresponding to the loess beds and higher insolation intensity corresponding to the paleosols.

The $\delta^{18}O$ curves show a steady increase in ice volume beginning early in MIS 5, and peak during MIS 2. The deep-sea $\delta^{18}O$ curves show higher ice volumes during MIS 2 than MIS 4 and, in ODP 677, a slight reduction in global ice volume during interstadial MIS 3. This corresponds very well with the grain size and susceptibility profiles at Wupu and Yanchang. The grain size variations show more abrupt changes during the last glaciation, although differences in sample resolution of the deep-sea and loess records may, in part, explain differences in the magnitude of the changes.

Both $\delta^{18}O$ and insolation variations show a

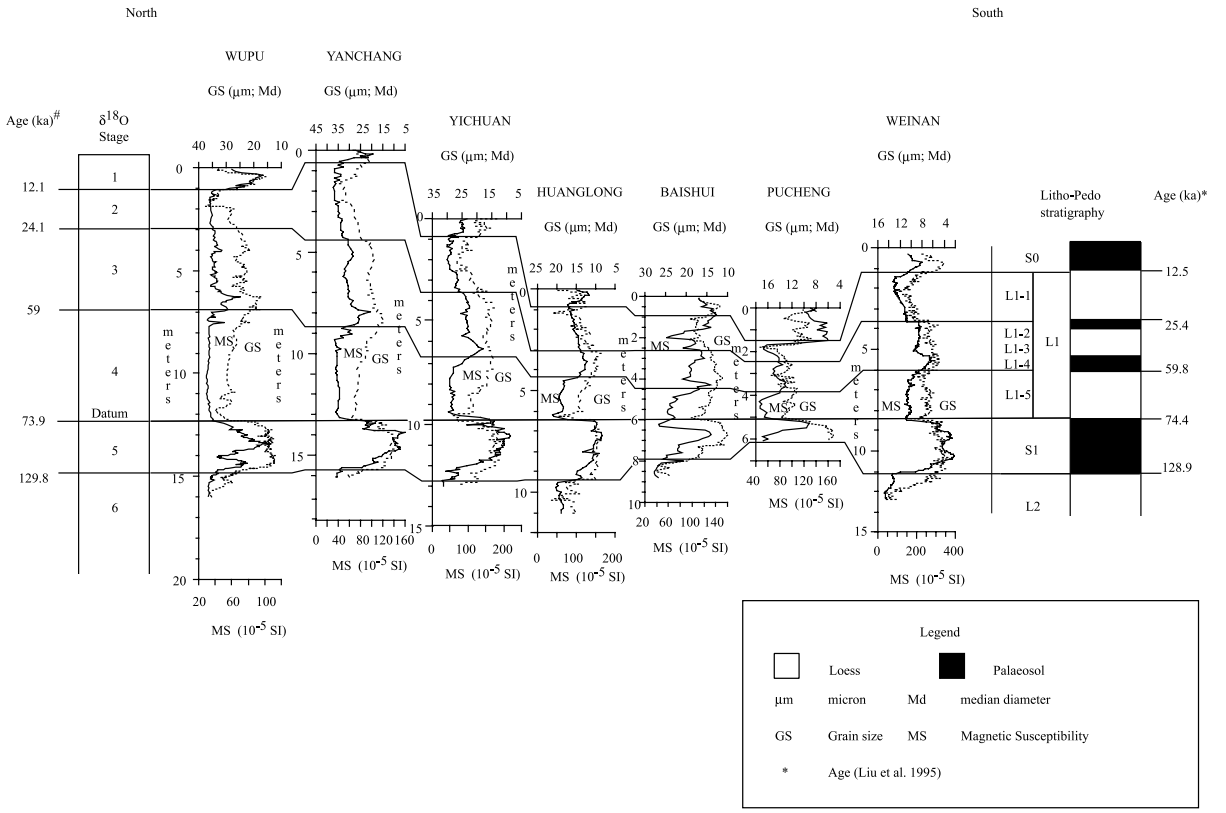

Fig. 3. Stratigraphic cross-section from the central Loess Plateau showing the continuity of the strata along the north to south transect. All locations use the same vertical scale (in meters). Magnetic susceptibility values are carbonate-free.

strong correlation with loess grain size and accumulation rate. A temporal comparison of grain size and accumulation rates clearly shows that loess grains are coarser and beds thicker in glacial units as compared to those deposited in interglacial units (Liu, 1985; An et al., 1991a,b; Ding et al., 1995; Shackleton et al., 1995; Vandenberghe et al., 1997). This is the basic temporal geologic and climatic model relating loess deposition to variations in insolation and global ice volume. In the next section we examine the two-component loess depositional model. In particular, variations in inferred loess grain size and accumulation rates for the last interglacial and glacial periods are examined and compared.

4. Loess depositional model

The Malan loess (L1; MIS 2–4) is subdivided into three loess members and two paleosols, based on field observations (Figs. 1 and 3). Vertically alternating loess and paleosols reflect variations in the rate of loess accumulation along a shifting climatic gradient (Pye, 1987; Pye and Tsoar, 1987). The Malan loess generally thins southward along the transect and thickens along the flank of the Qinling Mountains (Figs. 1 and 3). The architecture of the correlations is consistent and suggests a relatively consistent wind direction during deposition of the Malan loess.

The Malan loess exhibits a southward decrease in grain size (Liu and Chang, 1964). Lateral variations in grain size in the Malan reflect proximity to the desert source (Ding et al., 1999). In the desert–loess transition zone near Yulin (Figs. 1 and 4), Sun et al. (1995) show that there were at least three periods of desert expansion and two periods of desert contraction during the last interglacial–glacial cycle. Thus, lateral variations in

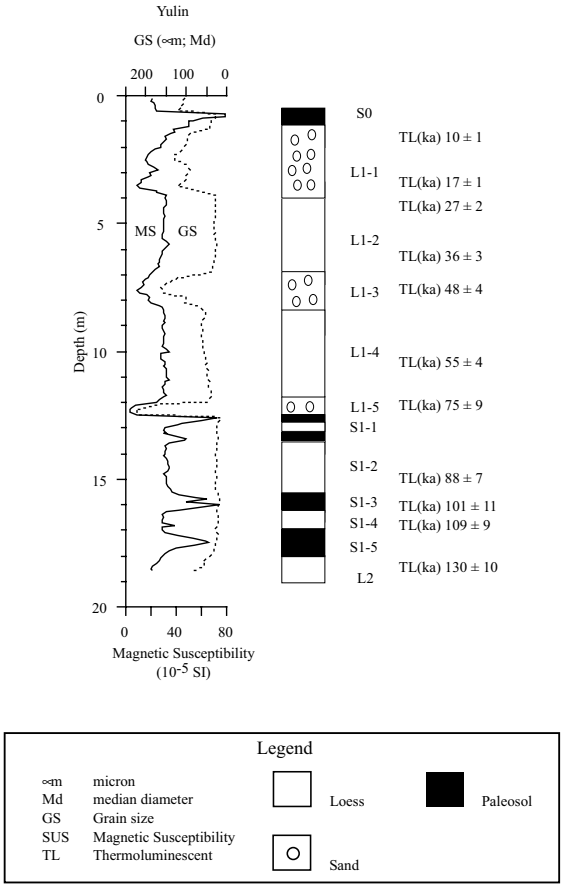

Fig. 4. The record of the last glacial desert–loess transition zone at the Yulin site (Sun et al., 1995).

grain size are, in part, coupled to the relative movement of the desert margin.

The peak median diameter of loess (Fig. 5a) displays a relatively steady increase northward toward the source during both the last interglacial and glacial periods. The general decline in the median diameter of loess evident in both glacial and interglacial units at all sites along the transect has the effect of shifting similar grain size means southward along the glacial set compared to the interglacial set, e.g. Yulin interglacial and Yichuan glacial (both 28 μm), and Yichuan interglacial (14 μm) and the closely similar Weinan glacial. These similarities in loess median grain size add a subtle dynamic and spatial qualification to the prevalent temporal model in which coarser loess grain size is directly attributed to glacial periods and finer loess to interglacial periods. The effect of variations in global ice volume on loess deposition, therefore, is to alter the distribution of loess grains through desert expansion and contraction, rather than to influence loess grain size directly.

Loess is generally thickest and accumulation rates highest near the source in both the last glacial and interglacial units (Fig. 5b). However, there is no evidence that glacial loess units are consistently thicker (Rokosh, 2001) or show high-

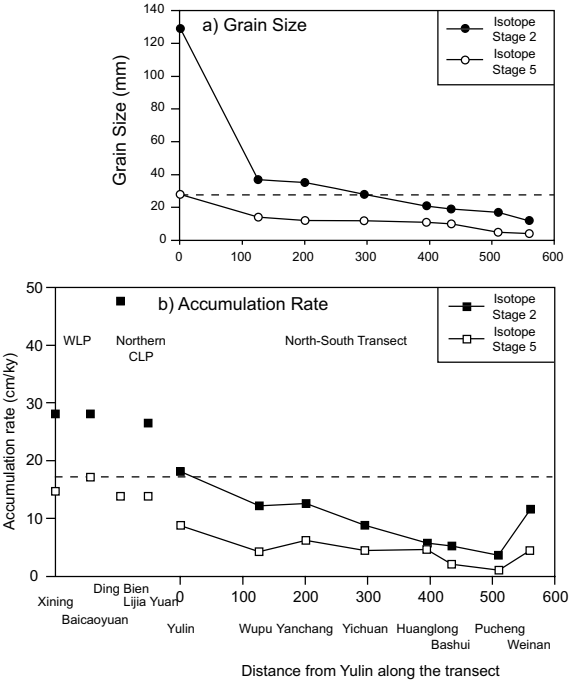

Fig. 5. (a) Grain size variations along the north–south transect on the eastern edge of the Central Loess Plateau (CLP). See Fig. 1 for the site locations. (b) Variations in the rate of loess accumulation along the transect. A few sites at the northern and northwestern margins of the CLP are included, along with sites from the Western Loess Plateau (WLP). Data from Rokosh (2001). Loess accumulation rates are regarded as minimum rates because of the difficulty in quantifying the extent of deflation within a loess bed. Dashed lines indicate the maximum grain size and accumulation rates in interglacial units. Publications used to estimate the thickness of the deposits are: Yulin, Sun et al. (1995, 1998); Lijia Yuan and Ding Bien, Dr. N.W. Rutter, personal communication; Baicaoyuan, Evans and Heller (1994) and Hunt et al. (1995); Xining, Hunt et al. (1995); all other locations, Rokosh (2001).

er accumulation rates than interglacial loess units. For example, loess accumulation rates (using the MIS 1/2, 4/5 and 5/6 boundaries of Liu et al., 1995) were higher during the last interglacial period (S1; MIS 5) at Yulin, Ding Bien, Lijia Yuan, Xining and Baicaoyuan than is recorded in most glacial loess units in the southern Loess Plateau (Figs. 1 and 5). This suggests that both the thickness and accumulation rate of glacial and interglacial loess reflect, in part, proximity to the source. In contrast, the temporal model suggests that loess accumulation rates were higher during glacial periods than interglacial periods. However, this observation is derived by comparing loess accumulation rates from sediments deposited relatively close to the source (during a glacial period) with loess deposited distal from the source (during an interglacial period). Thus, the temporal depositional model does not accurately reflect regional (i.e. spatial) variations in loess thickness or accumulation rates.

However, the reconstruction of the desert–loess depositional system is incomplete, because sediment proximal to the last interglacial desert margin and sediment distal from the last glacial desert margin have not been located (Rokosh, 2001). For this reason proximal grain size and accumulation rates during the last interglacial and glacial periods cannot be compared. Nonetheless, the present results suggest that, for the last interglacial–glacial cycle, variations in loess grain size and accumulation rates may have been influenced by climatic or non-climatic factors other than, or in addition to, desert migration and global ice volume variations. Some of the factors that affect modern loess deposition are examined below as a means of gaining insight into past processes that may have operated on the Loess Plateau.

5. Modern dust deposition

Modern dust accretion in North China occurs largely during dust storms of 'calm' events (Deere, 1984; Zhang et al., 1992, 1999). Dust storms in the Loess Plateau occur most frequently during April and May, and to a lesser extent during autumn (Ing, 1972; Deere, 1984; Liu, 1985; Littmann, 1991; Middleton, 1991; Merrill et al., 1989; Zhang et al., 1992; Mitsuta et al., 1995). There is also evidence (based on recent measurements) that appreciable dust falls occur all year round in North China, especially north of the northern margin of summer monsoon penetration, with a broad set of maxima in the summer half of the year (Derbyshire et al., 1997). According to Littmann (1991), dust storms in North China from 1976 to 1986 were associated with cold surges (see also Pye, 1987) during the spring, emanating from the high Arctic (Ren et al., 1985; Chang, 1987; Murakami, 1987). Dust storms are also associated with winter cold surges (Littmann, 1991), but at present in North China the winter storms are less frequent than those in spring (Merrill et al., 1989; Littmann, 1991). Hence, at present loess deposition in the Loess Plateau largely occurs after the aric winter monsoon retreats (e.g. late March; Chang, 1987), and prior to the onset of the wet summer monsoon (e.g. about mid-July; Tao and Chen, 1987) at a time when the Siberian high pressure system is relatively weak or absent (Barry and Chorley, 1968; Littmann, 1991; Chang, 1987).

Three main factors govern the potential for loess deposition (Tsoar and Pye, 1987). These are: (1) the availability of loess, (2) the frequency, magnitude and direction of loess transporting winds, and (3) a suitable sediment trap. In the modern record in China, the dust storm maxima, according to Littmann (1991), correspond to periods of low soil water storage during the spring, when evapotranspiration and surface heating are at a maximum (Gillette, 1986; Littmann, 1991). The spring maxima in dust storm frequency (from 1976 to 1986; Littmann, 1991) show a very weak correlation with mean monthly temperature ($r = -0.03$), a positive correlation with evaporation ($r = 0.31$), and an inverse correlation with both surface atmospheric pressure ($r = -0.46$) (see also Pye, 1987), and mean monthly precipitation ($r = -0.26$) (Littmann, 1991). Furthermore, there is no correlation between the seasonal strength of winds and dust storm frequency (Littmann, 1991). The strongest winds at present occur during the winter in China, while dust storms are most frequent during the dry spring. At present,

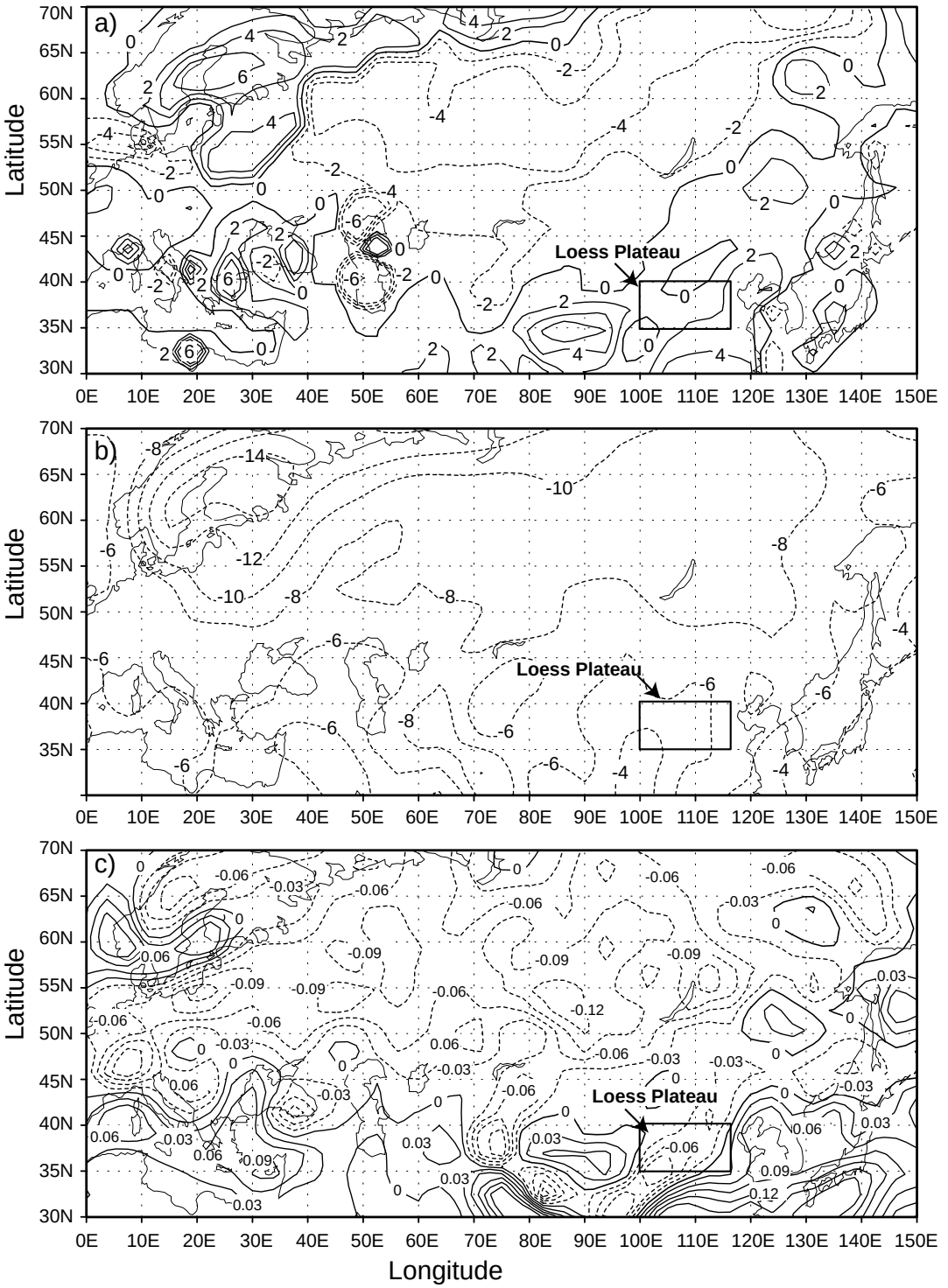

Fig. 6. Results from numerical GCM experiments for the LGM and the present day. Differences are all LGM minus present-day. (a) Difference in annual mean soil moisture content; values are in cm of water and the field saturation value is 15 cm. (b) Difference in annual mean temperature near the surface, in °C. (c) Difference in annual mean precipitation, in cm/day.

therefore, soil moisture content exerts a strong influence on the availability of dust in China for re-sedimentation in the Loess Plateau.

6. Soil moisture content during the last glaciation

Based on a multi-criteria approach (palynologic, pedogenic, paleocryogenic, paleoecologic), Velichko (1984) determined that continental Siberia at the LGM was cooler and drier than at present, whereas the Asian east coast was wetter. According to Velichko (1984), the Scandinavian Anticyclone (related to the north-Eurasian ice sheets), along with the Siberian and Polar anticyclones 'merged' (to a degree), leading to a cooler and drier climate in East Asia. Results from a numerical simulation of the LGM with a coupled atmosphere–ocean GCM (Bush and Philander, 1999) indicate that, according to the soil moisture content, the Asian continental interior was drier at the LGM whereas the east coast tended to be wetter (Fig. 6a). This pattern of soil moisture difference is thus in good agreement with that presented by Velichko (1984). Diagnosis of the model output indicates that annual mean surface temperatures were lower than those of today in the continental interior compared to those along the east coast (Fig. 6b). Temperatures were lower in the deep interior both because of downstream cooling induced by the Fennoscandian ice sheet, and because of the great distance to the oceans. A consequence of this pattern of cooling was that the hydrological cycle in the continental interior was weakened, leading to less available moisture in the atmosphere. In addition to this, the Fennoscandian ice sheet induced large-scale atmospheric subsidence downstream of its leeward margin, thereby suppressing precipitation over a large portion of the continental interior. This situation prevailed until the winds reached the east coast, where precipitation increased relative to that of the present (Fig. 6c).

As indicated in Fig. 6, the Loess Plateau is located along the boundary between drier and wetter regions. The desert margin would have been sensitive to these changes in its surface hydrology, through dune destabilization or stabilization by vegetation (Bagnold, 1941). This would also have been true of loess distribution on the plateau. These results suggest that non-local effects (i.e. the Fennoscandian ice sheet and the atmospheric circulation pattern that it induced to leeward) may well have influenced migration of the desert margin and hence loess deposition in East Asia. The link between ice volume and paleo-loess deposition in China, therefore, involved desert expansion or contraction, conceivably as a result of changes in soil moisture during relatively dry glacials and wet interglacials.

7. Discussion

The interpretation of climate mechanisms that forced a change in loess deposition during the last interglacial–glacial cycle must account for at least four observed stratigraphic and sedimentological characteristics of the succession in the Loess Plateau, as follows. (1) The stratigraphic alternation of sand, loess and paleosols involves variations in the rate of sediment accumulation along a shifting climatic gradient (Pye, 1987; Pye and Tsoar, 1987). (2) Loess beds are thickest and accumulation rates are highest near the desert source in sedimentary units laid down during both glacial and interglacial periods. Glacial loess beds are not exclusively thicker with higher accumulation rates than interglacial loess beds. However, the thickness of glacial and interglacial loess beds cannot be compared along the entire desert–loess depositional system, because of a lack of sites both near the interglacial desert source and distal from the last glacial source. (3) Glacial and interglacial loess units show similar grain size variations in space, although the distribution of the sizes varies because of the effects of desert expansion and contraction. (4) Temporal records of loess show coarser mean grain sizes for loess of glacial periods compared to the interglacial periods in response to desert expansion and contraction.

Alternations of loess and paleosols during the last interglacial–glacial cycle on the Loess Plateau were driven by variations in the rate of dust accretion (high near the desert source; low distal from the source) along a regional climatic gra-

dient. This gradient broadly shifted southward during glacial periods and northward during interglacial periods.

Vertical and lateral variations in grain size are related to ice volume variations through desert migration. Lateral variations in loess grain size are, in part, a function of proximity to the desert source (Ding et al., 1999), while vertical grain size trends appear to reflect desert expansion and contraction. Variations in regional accumulation rates are difficult to explain solely by climatic forcing. At present there does not seem to be any consistent relationship between loess accumulation rates and insolation or global ice volume variations (Rokosh, 2001). Other climatic or non-climatic factors that may affect rates of loess deposition must be considered (Rokosh, 2001), such as: (1) regional ice volume variations (Benn and Owen, 1998; Svendsen et al., 1999) that reach maxima prior to the LGM of the Laurentide and Scandinavian ice sheets; (2) variations in the rate and methods of silt production during glacial and interglacial periods (Reizebos and Van Der Wall, 1974; Smalley, 1995; Wright et al., 1998); (3) multiple source areas (Fang et al., 1999); (4) glacial winds may be more persistent than interglacial winds, but not necessarily of higher velocity (Phillips et al., 1993); (5) erosion, especially at warm to cold climate transitions; and (6) variations in soil moisture in the source and depositional areas (Bagnold, 1941; Velichko, 1984; Rea, 1994).

With respect to soil moisture, it is clear that in modern records low soil moisture values show a consistently positive relationship with increases in the frequency of dust storms. This may imply that there were more dust storms during the last glacial period than in the last interglacial period. However, it is yet to be clearly demonstrated that an increase in the number of dust storms led to an increase in the dust deposited in the Loess Plateau during the last glaciation.

8. Conclusion

Temporal records of loess grain size, thickness and accumulation rates for the last interglacial–glacial cycle do not accurately reflect regional spatial variations in these properties. Specifically, the temporal model of coarser grain sizes and thicker loess units during glacial periods than in interglacial periods is not applicable to both spatial and temporal components of loess properties. Interpretations of climatic forcing of the paleomonsoons have been largely based on observations of temporal changes in grain size and accumulation rates and do not accurately reflect the regional climatic or geologic influences on loess deposition.

The expansion and contraction of the desert source results in a change in the distribution of loess. Primary vertical or temporal changes in loess grain size are related to ice volume variations through shifts in the climatic gradient that result in desert expansion and contraction, while lateral variations in grain size, in part, reflect proximity to the source (Ding et al., 1999). However, the movement of the desert margin was due, in part, to variations in the Fennoscandian ice sheet that also affected East Asian wind patterns (Velichko, 1984; Bush and Philander, 1999) and induced changes in soil moisture. Thus, loess grain size variations in China are indirectly influenced by both regional and global ice volume variations. Variations in the thickness or accumulation rates of loess are not directly related to variations in insolation or global ice volume variations, and may correspond to other climatic or non-climatic factors.

Acknowledgements

This paper is a contribution of the Canadian Climate System History and Dynamics (CSHD) program supported by funding from the Natural Sciences and Engineering Research Council of Canada (NSERC) and the Atmospheric and Environment Service (AES) of Canada to N.W.R. Work by A.B.G.B. is supported by NSERC Grant OGP0194151 and NSERC-funded CSHD program funding was also provided by the National Natural Science Foundation of China. The first author would like to thank the reviewers, Dr. E. Derbyshire and Dr. F. Heller, for their

substantial contribution in improving the content and grammar of this manuscript. I have learned much from them. Their efforts are greatly appreciated.

References

An, Z.S., Wu, X., Wang, P., Wang, S., Sun, X., Lu, Y., 1991a. An evolution model for palaeomonsoon of China during the last 130,000 years. In: Liu, T.S. (Ed.), Quaternary Geology and Environment in China. Science Press, Beijing, pp. 37–244.

An, Z.S., Kukla, G., Porter, S.C., Xiao, J.L., 1991b. Late Quaternary dust flow on the Chinese Loess Plateau. Catena 18, 125–132.

Bagnold, R.A., 1941. Physics of Blown Sand and Desert Dunes, 1954 edn. Methuen, London, 265 pp.

Barry, R.G., Chorley, R.J., 1968. Atmosphere, Weather and Climate. Methuen, London.

Bassinot, F.C., Labeyrie, L.D., Vincent, E., Quidelleur, X., Shackleton, N.J., Lancelot, Y., 1994. The astronomical theory of climate and the age of the Brunhes-Matuyama magnetic reversal. Earth Planet. Sci. Lett. 126, 91–108.

Benn, D.I., Owen, L.A., 1998. The role of the Indian summer monsoon and the mid-latitude westerlies in Himalayan glaciation; review and speculative discussion. J. Geol. Soc. Lond. 155 (Part 2), 3535–3563.

Berger, A., Loutre, M.F., 1991. Insolation values for the climate of the last 10 million years. Quat. Sci. Rev. 10, 297–317.

Bush, A.B.G., Philander, S.G.H., 1999. The climate of the Last Glacial Maximum: results from a coupled atmosphere-ocean general circulation model. J. Geophys. Res. 104, 24509–24525.

Chang, B.K., 1987. Short- and long-range monsoon prediction in Southeast Asia. In: Fein, J.S., Stephens, P.I. (Eds.), Monsoons. Wiley, New York, pp. 579–606.

Deere, Z., 1984. Synoptic-climatic studies of dust fall in China since historic times. Sci. Sin. (Ser. B) 27, 825–836.

Derbyshire, E., Meng, X.M., Kemp, R.A., 1997. Provenance, transport and characteristics of aeolian dust in western Gansu province, China, and interpretation of the Quaternary loess record. J. Arid Environ. 39, 497–516.

Ding, Z.L., Liu, T.S., Rutter, N.W., Yu, Z.W., Guo, Z.T., Zhu, R.X., 1995. Ice-volume forcing of East Asian winter monsoon variations in the past 800,000 years. Quat. Res. 44, 149–159.

Ding, Z., Sun, J., Rutter, N.W., Rokosh, D., Liu, T., 1999. Changes in the sand content of loess deposits along a north to south transect of the Chinese Loess Plateau and the implications for desert variations. Quat. Res. 52, 56–62.

Evans, M.E., Heller, F., 1994. Magnetic enhancement and paleoclimate study of a loess/paleosol couplet across the Loess Plateau of China. Geophys. J. Int. 117, 257–264.

Fang, X., Li, J., Van der Woo, R., 1999. Rock magnetic and grain size evidence for intensified Asian atmospheric circulation since 800,000 years B.P. related to Tibetan uplift. Earth Planet. Sci. Lett. 165, 129–144.

Gillette, D.A., 1986. Dust production by wind erosion: necessary conditions and estimates of vertical fluxes of dust and visibility reduction by dust. In: Farouk, E.-B., Hassan, M.H.A. (Eds.), Physics of Desertification, Martinus Nijhoff, Dordrecht, pp. 361–371.

Hunt, C.P., Banerjee, S.K., Han, J.M., Solheid, P.A., Oches, E., Sun, W.W., Liu, T.S., 1995. Rock-magnetic proxies of climate change in the loess-Palaeosol sequences of the western Loess Plateau of China. Geophys. J. Int. 123, 232–244.

Ing, G.K.T., 1972. A dust storm over Central Asia, April 1969. Weather 27, 136–145.

Kukla, G.J., 1987a. Correlation of Chinese, European and American loess series with deep-sea sediments. In: Liu, T.S. (Ed.), Aspects of Loess Research. Ocean Press, Beijing, pp. 27–38.

Kukla, G., 1987b. Loess stratigraphy in central China and correlation with an extended oxygen isotope time stage scale. Quat. Sci. Rev. 6, 191–220.

Littmann, T., 1991. Dust storm frequency in Asia: climatic control and variability. Int. J. Climatol. 11, 393–412.

Liu, J., Nie, G., Chen, T., Song, C., Zhu, G., Li, K., Gao, Z., Qiao, Y., 1995. A preliminary high resolution time scale for the last 130,000 years at Weinan loess section. Sci. Geol. Sin. (Overseas edn.; Suppl. Issue), Beijing, China 1, 9–22.

Liu, T.S., 1985. Loess and the Environment. China Ocean Press, Beijing, 251 pp.

Liu, T.S., Chang, T.H., 1964. The 'Huangtu' (loess) of China. Report of the Sixth INQUA Congress, Warsaw, 1961, vol. 4, pp. 503–524.

Liu, T., Ding, Z., 1993. Stepwise coupling of monsoon circulation to global ice volume variations during the Late Cenozoic. Glob. Planet. Change 7, 119–130.

Merrill, J.T., Uematsu, M., Bleck, R., 1989. Meteorological analysis of long range transport of mineral aerosols over the North Pacific. J. Geophys. Res. 94, 8584–8598.

Middleton, N.J., 1991. Dust storms in the Mongolian People's Republic. J. Arid Environ. 20, 287–297.

Mitsuta, Y., Hayashi, T., Takemi, T., Hu, Y., Wang, J., Chen, M., 1995. Two severe local storms as observed in the arid area of Northwest China. J. Meteorol. Soci. Jpn. 73, 1269–1284.

Murakami, T., 1987. Effects of the Tibetan Plateau. In: Chang, C.P., Krishnamurti, T.N. (Eds.), Monsoon Meteorology. Oxford University Press, New York, pp. 235–270.

Phillips, F.M., Zreda, M.G., Ku, T.-L., Lou, S., Huang, Q., Elmore, D., Kubik, P.W., Sharma, P., 1993. $^{230}Th/^{234}U$ and ^{36}Cl dating of evaporite deposits from the western Qaidam Basin, China: implications for glacial-period dust export from Central Asia. Geol. Soc. Am. Bull. 105, 1606–1616.

Pye, K., 1987. Aeolian Dust and Dust Deposits. Academic Press, 334 pp.

Pye, K., Tsoar, H., 1987. The mechanics and geological implications of dust transport and deposition in deserts with par-

ticular reference to loess formation and dune sand diagenesis in the northern Negev, Israel. In: Frostick, L., Reid, I. (Eds.), Desert Sediments: Ancient and Modern. Geol. Soc. Spec. Publ. 35, pp. 139–156.

Rea, D.K., 1994. The paleoclimatic record provided by eolian deposition in the deep sea: The geologic history of wind. Rev. Geophys. 32, 159–195.

Reizebos, A., Van Der Wall, L., 1974. Silt-sized particles: a proposed source. Sediment. Geol. 12, 279–285.

Ren, M., Yang, R., Bao, H., 1985. An outline of China's physical geography. China Knowledge Series. Foreign Languages Press, Beijing, 471 pp.

Rokosh, D., 2001. Stratigraphy and palaeoclimatology of loess of the Loess Plateau China over the last Interglacial-Glacial cycle. Unpublished Ph.D. Thesis.

Shackleton, N.J., 1996. Timescale Calibration, ODP 667, International Geosphere Biosphere Program, Past Global Changes World Data Center-A for Paleoclimatology Data Contribution Series 96-018. National Oceanic and Atmospheric Administration/National Geophysical Data Center Paleoclimatology Program, Boulder, CO.

Shackleton, N.J., An, Z., Dodonov, A.E., Gavin, J., Kukla, G.J., Ranov, V.A., Zhou, L.P., 1995. Accumulation rate of loess in Tadjikistan and China: relationship with global ice volume cycles. Quat. Proc. 4, 1–6.

Shackleton, N.J., Berger, A., Peltier, W.R., 1990. An alternative astronomical calibration of the lower Pleistocene timescale based on ODP Site 677. Trans. R. Soc. Edinburgh Earth Sci. 81, 251–261.

Smalley, I., 1995. Making the material: the formation of silt-sized primary mineral particles for loess deposits. Quat. Sci. Rev. 14, 645–657.

Sun, J., Ding, Z., Liu, T., 1995. The environmental evolution of the desert-loess transition zone over the last glacial-interglacial cycle. In: Wang, S. (Ed.), Quaternary Geology and Past Environmental Changes in China. Science Press, Beijing, pp. 1–8.

Sun, J., Ying, G., Ding, D., Liu, T., Chen, J., 1998. Thermoluminescence chronology of sand profiles in the Mu Us Desert, China. Palaeogeogr. Palaeoclimatol. Palaeoecol. 144, 25–233.

Svendsen, J.I., Astakov, V.I., Bolshiyanov, D.Y., Demidov, I., Dowdeswell, J.A., Gataullin, V., Hjort, C., Hubberten, H.W., Larsen, E., Mangerud, J., Melles, M., Moller, P., Saarnisto, M., Siegert, M.J., 1999. Maximum extent of the Eurasian ice sheets in the Barents and Kara Sea region during the Weichselian. In: Larsen, E., Funder, S., Thiede, J. (Eds.), Late Quaternary history of northern Russia and adjacent shelves. Boreas 28, 234–242.

Tao, S., Chen, L., 1987. A review of recent research on the East Asian summer monsoon in China. In: Chang, C.P., Krishnamurti, T.N. (Eds.), Monsoon Meteorology. Oxford University Press, New York, pp. 60–92.

Tsoar, H., Pye, K., 1987. Dust transport and the question of desert loess formation. Sedimentology 34, 139–153.

U.S. Defense Mapping Agency Aerospace Center, 1987. Operational Navigation Chart, Sheets F-7, F-8, G-8, G-9, 4th edn. U.S. Department of Defense.

Vandenberghe, J., An, Z.S., Nugteren, G., Lu, H.Y., Van Huissteden, K., 1997. New absolute time scale for the Quaternary climate in the Chinese loess region by grain-size analysis. Geology 25, 35–38.

Velichko, A.A., 1984. Later Pleistocene spatial paleoclimate reconstructions. In: Velichko, A.A., Wright, Jr., H.E., Barnosk, C.W. (Eds.), Late Quaternary Environments of the Soviet Union. University of Minnesota, Minneapolis, MN, pp. 35–41.

Wright, J., Smith, B., Whalley, B., 1998. Mechanisms of loess-sized quartz silt production and their relative effectiveness: laboratory simulations. Geomorphology 23, 15–34.

Zhang, X., An, Z., Liu, D., Chen, T., Zhang, G., Arimoto, R., Zhu, G., Wang, X., 1992. Study on three dust storms in China-source characterization of atmospheric trace element and transport process of mineral aerosol particles. Chin. Sci. Bull. 37, 940–945.

Zhang, X.Y., Arimoto, R., An, Z.S., 1999. Glacial and interglacial patterns for Asian dust transport. Quat. Sci. Rev. 18, 811–819.